Mar Geophys Res
DOI 10.1007/s11001-012-9160-6

ORIGINAL RESEARCH PAPER

# Impacts of sediment supply and local tectonics on clinoform distribution: the seismic stratigraphy of the mid Pleistocene-Holocene Indus Shelf

**David R. Limmer · Timothy J. Henstock · Liviu Giosan · Camilo Ponton · Ali R. Tabrez · David I. M. Macdonald · Peter D. Clift**

Received: 10 January 2012 / Accepted: 20 July 2012


**Abstract** We present results from the first high-resolution seismic reflection survey of the inner Western Indus Shelf, and Indus Delta, Arabian Sea. The results show major regional differences in sedimentation across the shelf from east to west, as well as north to south, both since the Last Glacial Maximum ($\sim$20 ka) and over longer time scales. We identify 10 major regional reflectors, interpreted as representing sea level lowstands. Strong compressive folding is observed underlying a reflector we have called Horizon 6 in the north-western shelf, probably compression associated with the transpressional deformation of the Murray Ridge plate boundary. Downslope profiles show a series of well developed clinoforms, principally at the shelf edge, indicating significant preservation of large packages of sediment during lowstands. These clinoforms have developed close to zones of deformation, suggesting that subsidence is a factor in controlling sedimentation and consequently erosion of the Indus Shelf. These clinoforms fan out from dome features (tectonic anticlines) mostly located close to the modern shoreline.

**Keywords** Indus Delta · Quaternary · Clinoforms · Seismic stratigraphy

D. R. Limmer (✉) · D. I. M. Macdonald · P. D. Clift
School of Geosciences, University of Aberdeen,
Meston Building, Aberdeen AB24 3UE, UK
e-mail: d.r.limmer@abdn.ac.uk

T. J. Henstock
School of Ocean and Earth Science, National Oceanography Centre, University of Southampton,
Southampton SO14 3ZH, UK

L. Giosan · C. Ponton
Department of Geology and Geophysics, Woods Hole Oceanographic Institution, 360 Woods Hole Road,
Woods Hole, MA 02543, USA

A. R. Tabrez
National Institute of Oceanography ST-47 Block 1,
Clifton, Karachi 75600, Pakistan

*Present Address:*
P. D. Clift
Department of Geology and Geophysics, Louisiana State University, Baton Rouge, LA 70803, USA

## Introduction and regional background

The stratigraphy and morphology of clastic continental margins represents the integrated result of continental-margin subsidence, sediment supply, and the effects of sea level variation. Our understanding of how margins evolve through time was greatly advanced by the introduction of sequence stratigraphic concepts by Vail et al. (1977) and subsequent related refinements, such as Haq et al. (1987). These models focused on the impacts of sea level variations and tended to ignore the role of changing sediment supply or changing rates of basement tectonic subsidence. Moreover, these models tended to view the margin in a two dimensional fashion, ignoring lateral migration by delta lobes or the role of submarine canyons. While it has been widely observed that the morphology and stratigraphy of continental shelves reflect the interplay among sea level, sediment supply, and oceanographic processes (e.g., Swenson et al. 2005; Porebski and Steel 2006; Pratson et al. 2007), the diversity of shelf architectures makes it difficult to isolate the relative importance of these processes and to develop general models of shelf stratigraphy. In areas of high sediment supply, such as deltas, processes on the delta plain and inner shelf can strongly influence mid- to outer-shelf areas (Greene et al. 2007; Reijenstein et al. 2011). At a larger

Published online: 01 August 2012

scale, these processes control the trajectories of shelf edge and shoreline (Henriksen et al. 2009). In this study we examined the Pleistocene–Recent evolution of a major river delta in a tectonically active setting with known temporal variations in sediment supply in order to determine how its stratigraphic development compares with the Vail model.

The Indus Shelf is located in the northern Arabian Sea on the northwest rifted margin of the Indian sub-continent (Fig. 1). The shelf is approximately 180 km wide from the delta to the shelf-slope break and stretches southeast from the Murray Ridge and Makran Coast to the Rann of Kutch in India. The shelf is dominated by the submarine delta of the 2,900 km long Indus River. The modern Indus Delta system has a compound clinoform morphology, whereby two separate deltas are present, the subaerial and subaqueous systems (Giosan et al. 2006); in this paper we focus on the subaqueous system. The Indus Shelf acts as both a conduit and a sink for sediment, principally delivered by the Indus River and a smaller fraction derived by aeolian processes from deserts during the winter monsoon (Sirocko and Lange 1991). The Indus Canyon runs from close to the modern river mouth toward the southwest and divides the shelf into two halves. The Indus Delta coast is exposed to the highest offshore wave energy of any delta (Wells and Coleman 1984) and received the fifth-largest sediment load prior to human intervention, mostly in the form of damming (Milliman and Syvitski 1992), which started in the early twentieth Century and has accelerated since the 1950s (Giosan et al. 2006). Thus the Indus is an end-member delta having both a high (if erratic) sediment supply and exposure to medium to high wave energy at the coast (Milliman et al. 1984; Jelgersma et al. 1993).

The deep-sea Indus Fan has been studied both over periods of $10^6$–$10^7$ years (e.g., Droz and Bellaiche 1991; McHargue 1991; Clift et al. 2001, 2002; Gaedicke et al. 2002; Deptuck et al. 2003) and over the Quaternary (e.g., Coumes and Kolla 1984; Kolla and Coumes 1987; Prins et al. 2000). In theory the deep-sea record could be used to reconstruct the evolving environment and erosional state in the onshore drainage basin. However, all sediment that reaches the deep oceans has to pass across coastal and shelf zones where sediment storage may occur, thus buffering the deep-sea record. Changes in relative sea level and climate can control delta development and strongly influence sediment supply from the shelf to the deep-sea fan. Furthermore, there can be long periods where rivers are not connected to the deep-sea fans depending on sediment

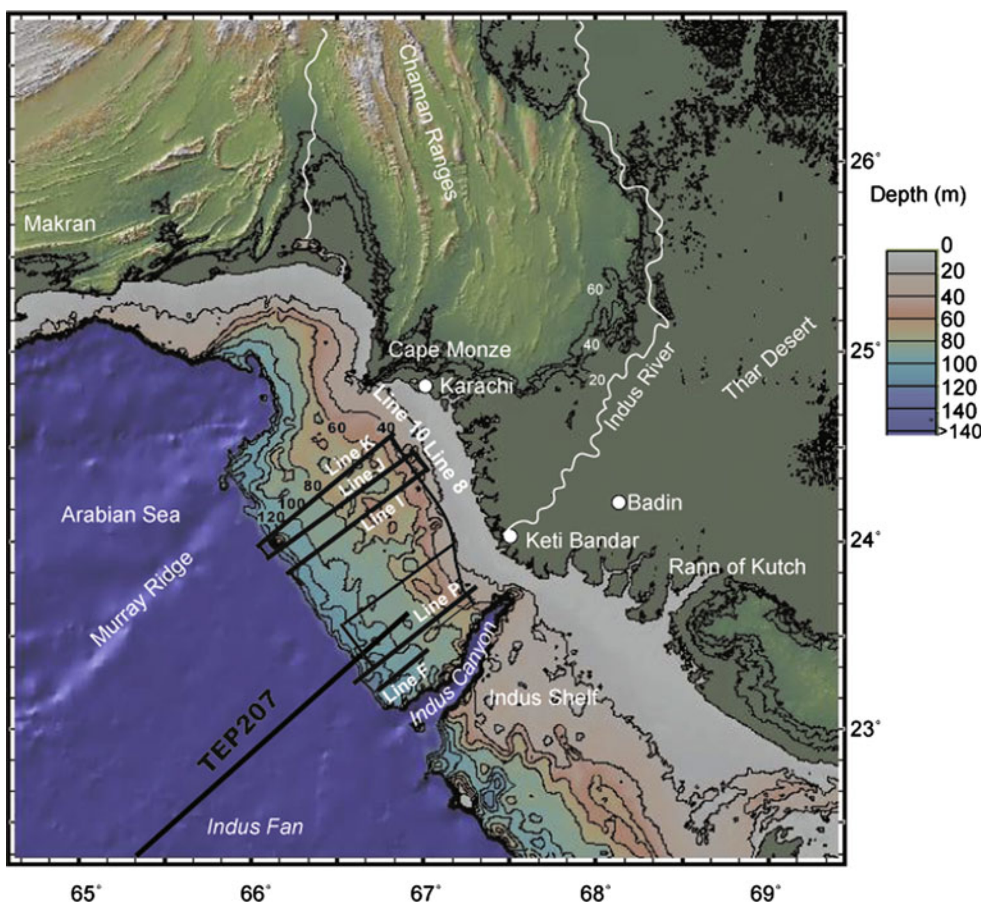


**Fig. 1** Regional bathymetric map showing the modern Indus Delta, Arabian Sea and other key features discussed in the text including Line TEP209. Bathymetry is from GeoMapApp

supply, shelf width, and volume (Burgess and Hovius 1998).

The long-term regional stratigraphy of the Indus Shelf can be understood from a combination of relatively deep-penetrating (several km) industry seismic data and wells (Clift et al. 2001). The shelf is mantled by around 500–700 m of Pleistocene sediments (Clift 2006), while the modern Indus Canyon is only the last of several that have been abandoned and infilled (Deptuck et al. 2003). Higher-quality, more recent surveys now reveal that the shelf west of the Indus Canyon is cut by a series of deep-penetrating normal faults, interpreted as growth faults (e.g., Line TEP207 on Fig. 1; Carmichael et al. 2009). A compilation of industry data was presented by Daley and Alam (2002) providing a chronostratigraphic model dating back 120 My and documented canyon incision and fill within the fan and slope between the Oligocene and Plio-Pleistocene.

The primary account of Quaternary sedimentation on the shelf comes from shallow-penetrating, high-resolution 'Parasound' seismic and bathymetric survey on the slope and shelf edge (von Rad and Tahir 1997). They showed a sediment-free outer shelf, contrasting with rapid sedimentation on the continental slope, and further deduced a decline in sediment supply during the Holocene. However, further inshore on the shelf the Indus River developed an asymmetric compound clinoform on both sides of the Indus Canyon during the Holocene (Giosan et al. 2006). A shallow delta front clinoform extends along the entire delta coast, west of the canyon, from the shoreline to 10–25 m water depth. The deeper mid-shelf clinoform (∼30 and

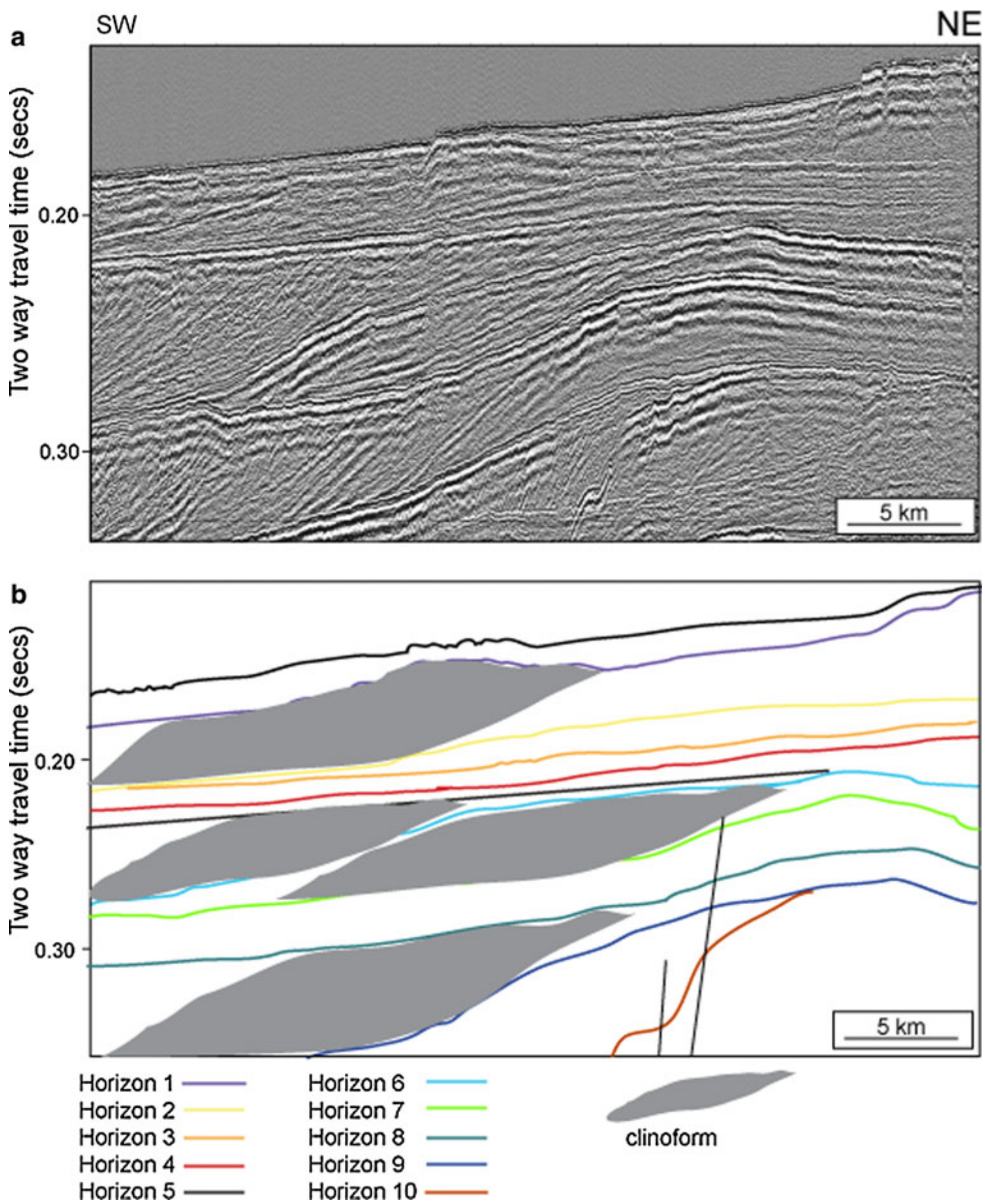


**Fig. 2** **a** Seismic image of Line F showing a compressional feature forming beneath Horizon 6, **b** interpretation of Line F showing area of probable clinoform development. See Fig. 1 for location

90 m water depth) has developed asymmetrically around the Indus Canyon with the eastern clinoform reaching farther onto the shelf than its western counterpart. Since 1978 the modern Indus River has gradually shifted east, with former distributaries now forming tidal creeks (Siddiqui and Maajid 2004). However, for much of the Holocene the delta was probably migrating in the opposite direction, away from the Thar Desert in the southeast to the modern location closer to Karachi (e.g., Kazmi 1984) suggesting that the locus of sediment supply to the shelf has changed over short periods of time, but also consistent with the long-term history outlined previously.

Here we examine the development of the submarine delta and shelf of the Indus River using high-resolution (1–2 m) medium penetration ($\sim$250–500 m beneath seabed) multichannel seismic reflection data. We target the submarine delta, continental shelf and upper slope, applying seismic-stratigraphic analysis to assess how sediment has been dispersed from the river mouth to the western parts of the shelf over a series of recent sea level cycles. The focus is the shelf west of the Indus canyon in an area where an active clinoform linked to the modern river mouth is developing. Because we have no deep coring control the ages of the imaged sequences remain unclear

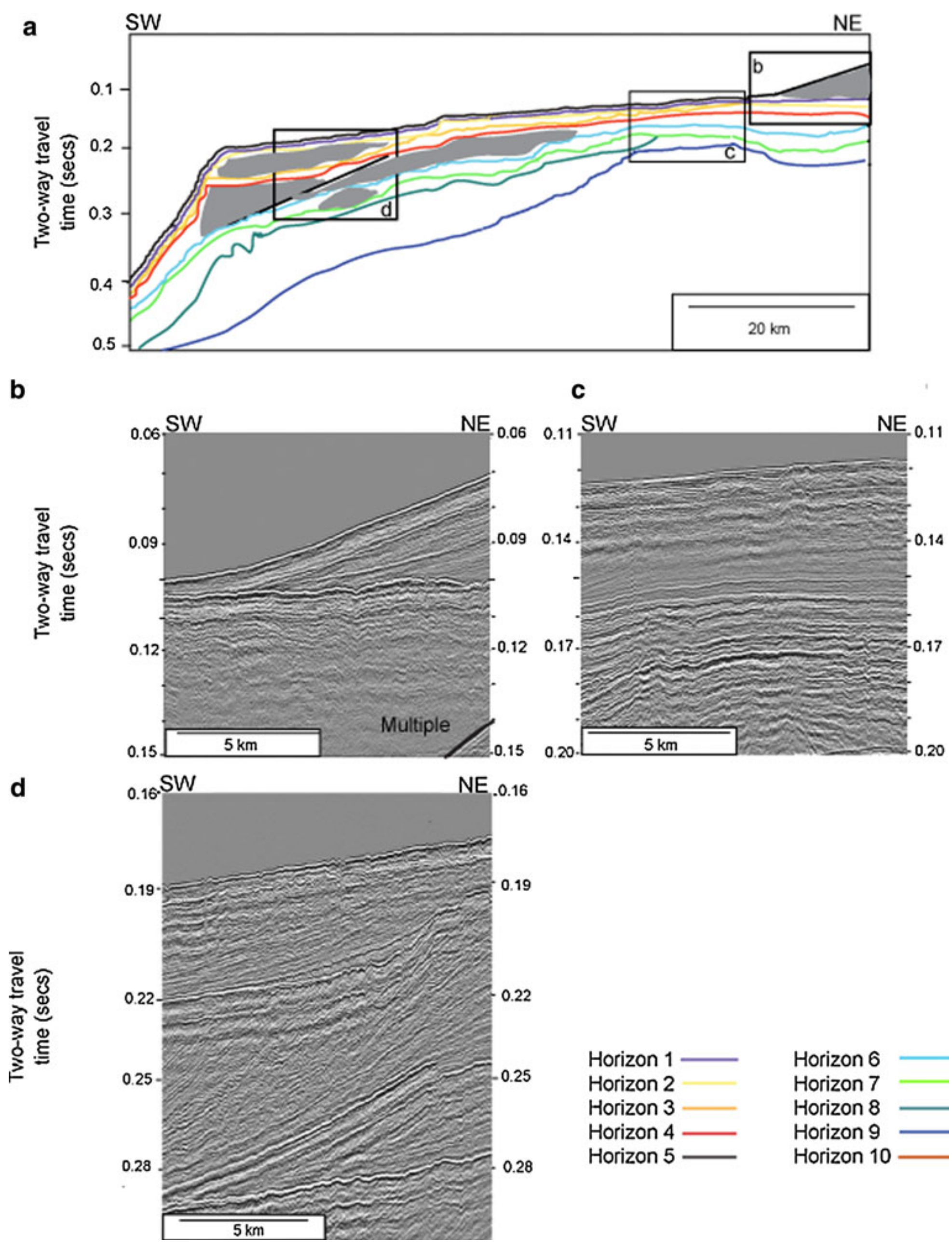


**Fig. 3** **a** Schematic diagram of Line P. An active clinoform, compressional features, ancient clinoforms and channel structures are all visible. **b** Active clinoform in Line P with a highly angular erosional base. **c** Uplifted block and slight deformation in the older horizons. **d** Buried clinoform forming between Horizons 6 and 7. See Fig. 1 for location

but are presumed to span the past few $10^5$ years based on earlier estimates of shelf stratigraphy (e.g., Clift et al. 2001). We further attempt to understand how the shelf edge has prograded over time and the principal controls that dictate the routing of sediment through the shallow shelf waters from the delta to the slope, and hence potentially to dispersal in the deep ocean. In addition to looking at clinoform development and relationships between sediment supply and sea level, this study also provides an opportunity to examine the Pleistocene-Recent passive margin stratigraphy of the Indus Shelf in higher resolution then has generally been completed previously.

## Methods

During Winter 2008/2009 the *RV Pelagia* collected approximately 1,500 km of seismic reflection data across the Indus Shelf on both sides of the Indus Canyon. The study area was chosen to extend inshore from that covered by von Rad and Tahir (1997). Seismic reflection data in this paper were collected using a Sparker source and a 60 channel, 100-m-long (60 m active) hydrophone streamer. The Applied Acoustic Engineering Squid 2000 Sparker system was powered by a 2200J CSP2200 source. The hydrophone was towed from the ship's A-frame and recorded on a Geometrics Strataview R60 seismograph and Marine Controller software. Data were stored on DDS4 tapes as 318,000 shot gathers in SEGD8058 format. Shots were synchronised to UTC from a GPS clock. Processing included geometry assignment, spherical divergence corrections, normal moveout (NMO) correction using velocities determined from iterative velocity analysis at 1–4 km spacing, and pre- and post-stack predictive deconvolution (Pinson 2010).

Seismic data were collected in a series of dip profiles at 20–30 km spacing, each of which runs seaward from approximately 30–40 km from the coast to cross the shelf break. We show seven lines of seismic data covering a total of ~360 km of Sparker seismic data from the western side of the Indus Canyon where the best data coverage was obtained. The lines include five oriented northeast-southwest downslope (Figs. 3, 4, 5, 6, 7), and two oriented northwest-southeast across the shallowest part of the survey (Figs. 8, 9).

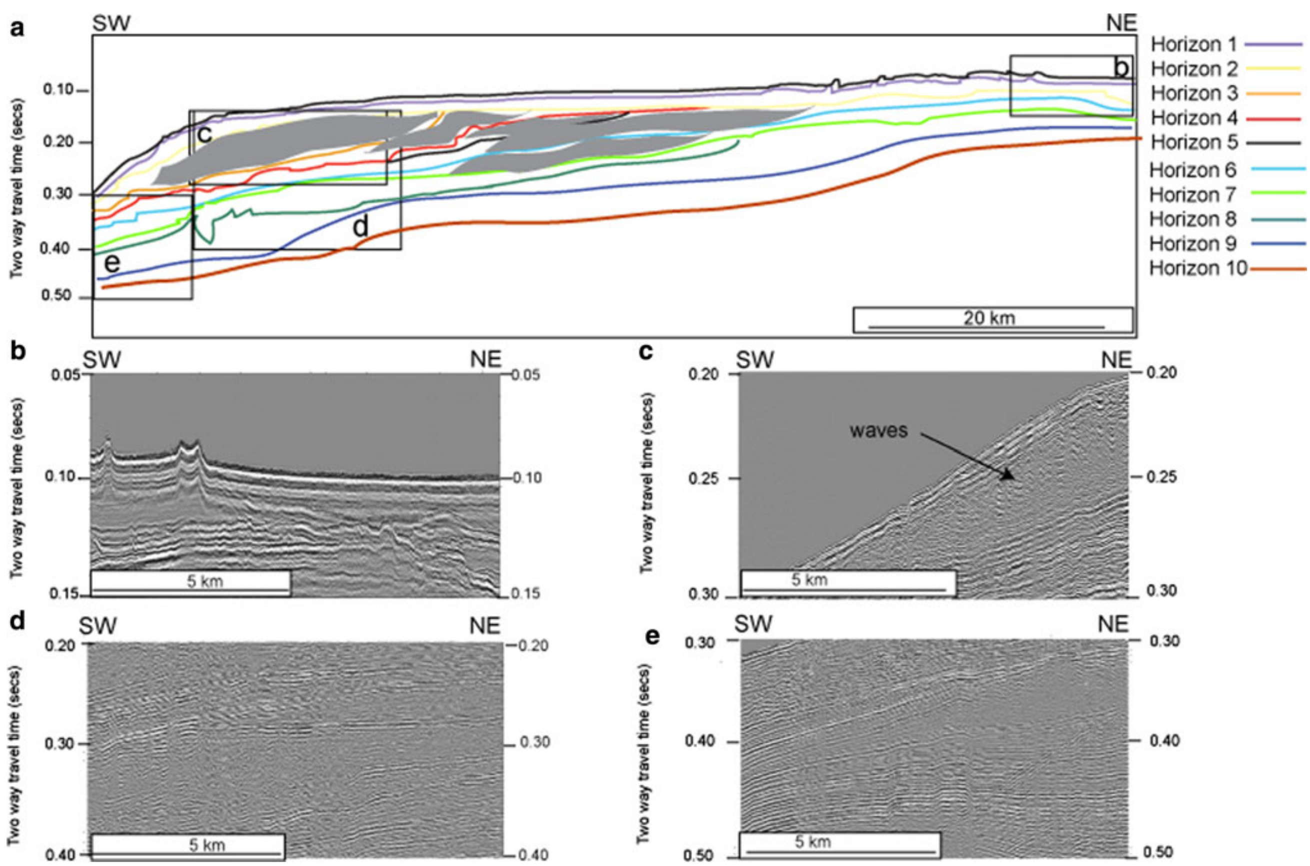


**Fig. 4** a Interpretation of Line I showing compression, channels and a aggrading (Horizons 9–5) to prograding (Horizons 5–1) clinoform sequences. **b** Nearshore surface of Line I showing slight deformation but no modern clinoform. **c** A series wavy structures forming on the slope (see *arrow*). **d** The edge of the slope showing a prograding clinoform sequence and steep narrow channels. **e** The slope edge showing slight uplift at depth and further wave structures on the slope. See Fig. 1 for location

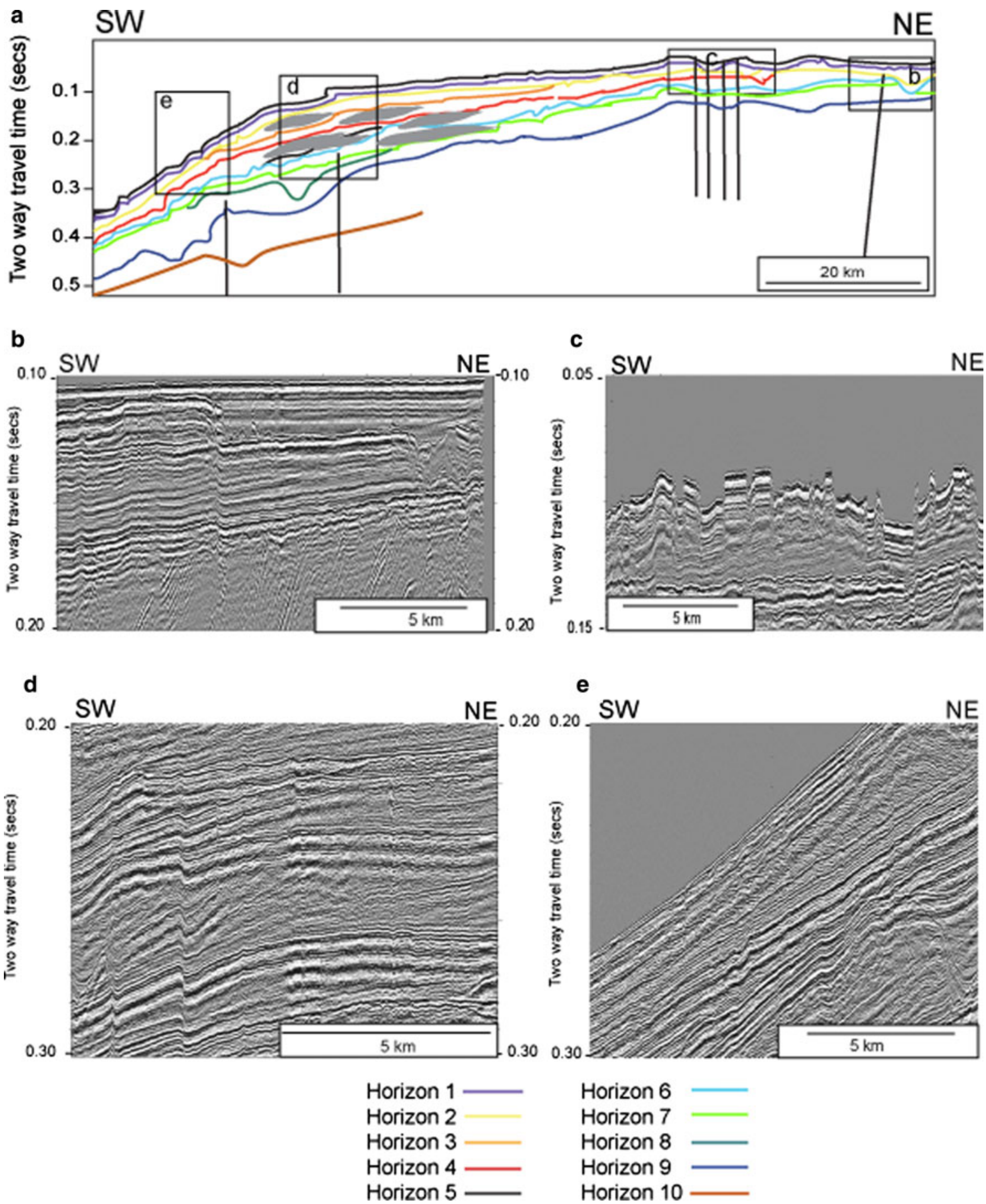


**Fig. 5** a Interpretation of Line J showing possible channel formation a more aggradational clinoform sequence with additional deformation on the slope and near surface faulting. **b** Series of ancient channel formed within 30 km of the modern shoreline. **c** Further deformation visible at the surface which includes some faults penetrating all visible horizons. **d** The same clinoform observed in Lines P and I between Horizons 6 and 7 which appears to have slumped due to faulting on the slope. **e** The shelf edge, showing the toe of some clinoforms and no wave features. See Fig. 1 for location

Sediment thickness was calculated using Kingdom software by converting horizon data to isochrons, which were converted to isopach maps assuming constant internal velocity of 1,600 m/s, based on unpublished data measured on ~10 m long sediment cores within the study area.

## Results

The sloping shelf edge and Indus Canyon are clearly visible in the regional bathymetry (Fig. 1). The main structures visible on the shelf are a series of clinoforms (e.g.

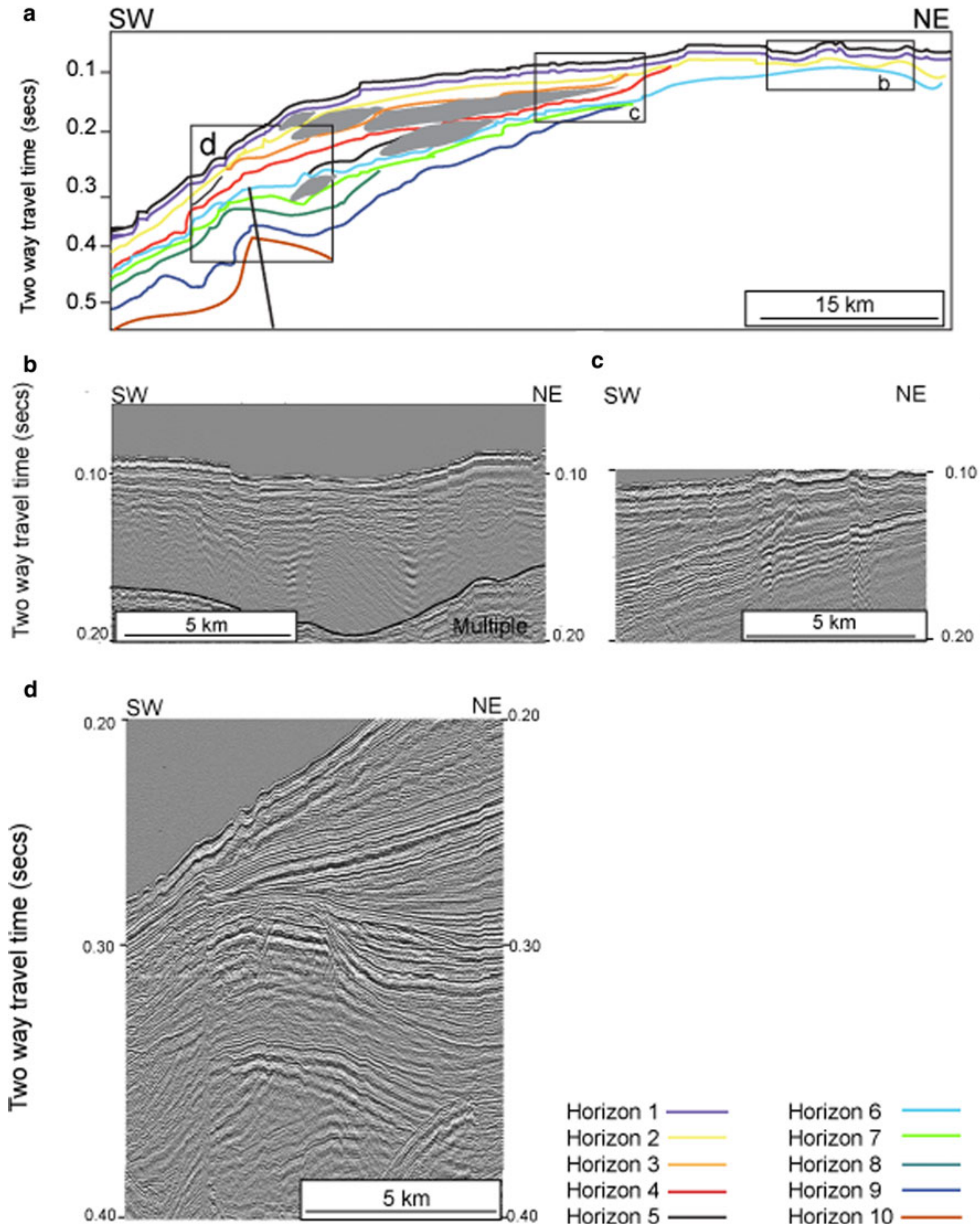


**Fig. 6** **a** Interpretation of Line K, the most northwestern line discussed, showing a complex clinoform sequence which only prograded between Horizons 4 and 1. **b** Subsurface folding close to the modern shoreline. **c** Fanning out of stratigraphy along the slope in Line K. **d** Sequence of stacked clinoforms formed above an uplifted block. See Fig. 1 for location

Line F Fig. 2a, b). At Line F, located in the east of the study region, these appear to develop from a doming structure observed below 0.25 s two-way time (TWT). These doming structures are also common throughout the study area. In Line P, an 83 km long section, 30 km northwest of Line F a much larger hump-shaped feature is visible below 0.23 s. TWT, spanning most of the section (Fig. 3c). Above these doming structures a shallower clinoform is observed at the seabed (Fig. 3b) which has developed much closer to the modern shoreline in Line P.

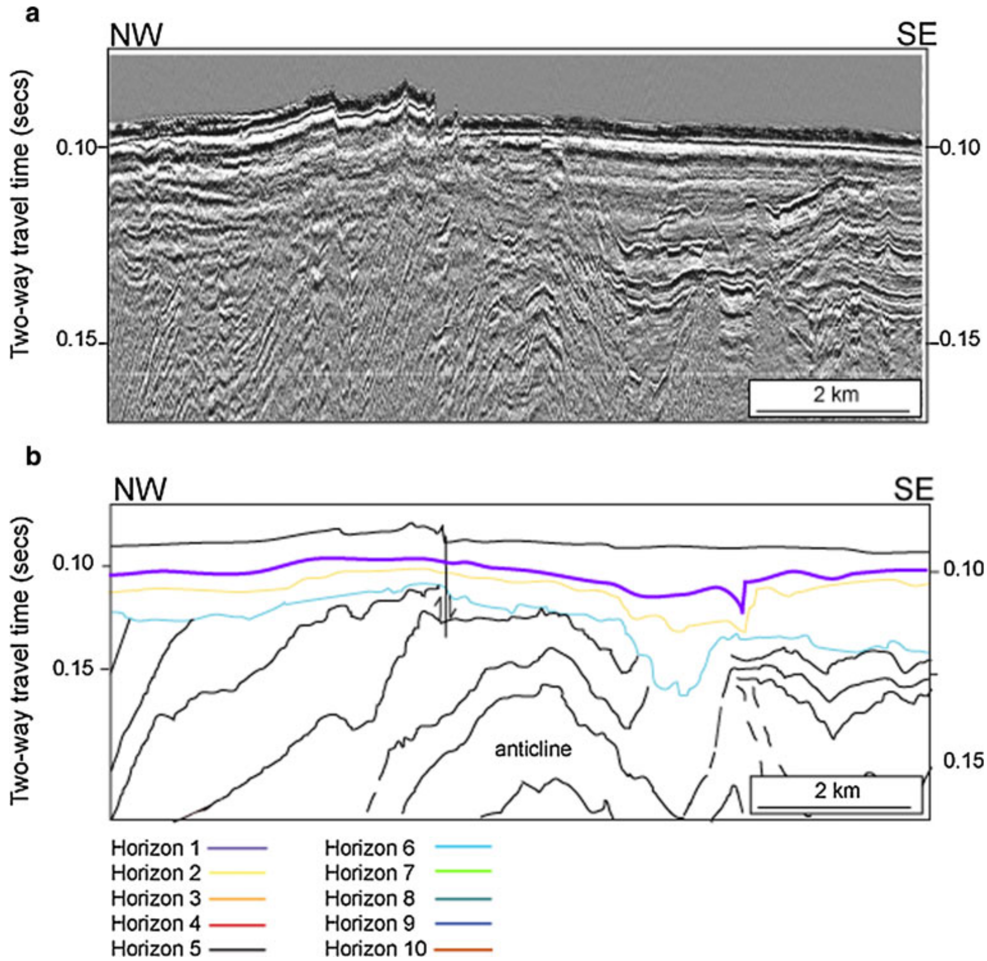


**Fig. 7** **a** Image of Line 10 seismic showing channelization and slight uplift to the west. Deformation is clearly visible beneath Horizon 6. **b** Interpretation of Line 10 showing clear tectonic folding beneath Horizon 6. See Fig. 2 for location

The deeper clinforms appear to fan out from the dome structure (Fig. 3d). However, the clinoform at the seabed does not appear to be related to any doming structure.

In the north-western shelf Line I (Figs. 1, 4) is located approximately 80 km northwest of Line P. The modern Indus clinoform is no longer visible in Line I, and is replaced by a thin layer of sediment on the surface which appears to be uplifted (Fig. 4b) in the form of a dome feature. Unlike along Line P, this deformation has affected the modern sea floor along Line I (Fig. 4b). Again, a series of clinoforms are present and appear to prograde out toward the slope (Fig. 4c–e). Some have prograded at least 20 km along the shelf. The boundaries between these clinoforms are generally smooth in the central shelf, but at the slope, boundaries become increasingly irregular (Fig. 4d, e). At the slope some slight uplift appears to be present below 0.4 s, possibly faulted (Fig. 4e). Although the major depositional features observed throughout the study area are clinoforms, a series of wavy structures can also be seen on the $\sim 1°$ dipping slope throughout the study area. These are clearly visible on the slope of Line I between 0.2 and 0.3 s, thinning slightly downslope (Fig. 4c).

In the far northwest, 15 km west of Line I deformation on the slope appears to be more intense in Line J and Line K (Figs. 5, 6) when compared to either Line I or Line P. Narrow channels, now infilled, are found to the NE end of Line J (Fig. 5b). However, the clinoform is thinner than along Line I. Other clinoforms are developed on the slope (Fig. 5d, e). The clinoforms in this region appear smaller than those observed further east, although fanning away from dome structures is still observed (Fig. 6c). Minor faulting is also observed across the section (Fig. 5b–d). In Line 10 (Fig. 7) and Line 8 (Fig. 8) subsurface deformation is still present together with folding observed at depth in the northwest corner of the study area (Fig. 6b, d).

Channel incision and fill is seen at the slope edge in Line I (Fig. 4d, e) and occurs commonly on the slopes of these north-western shelf lines. It is also observed closer to the coastline in Line J (Fig. 5b), Line 10, and Line 8. Line 10

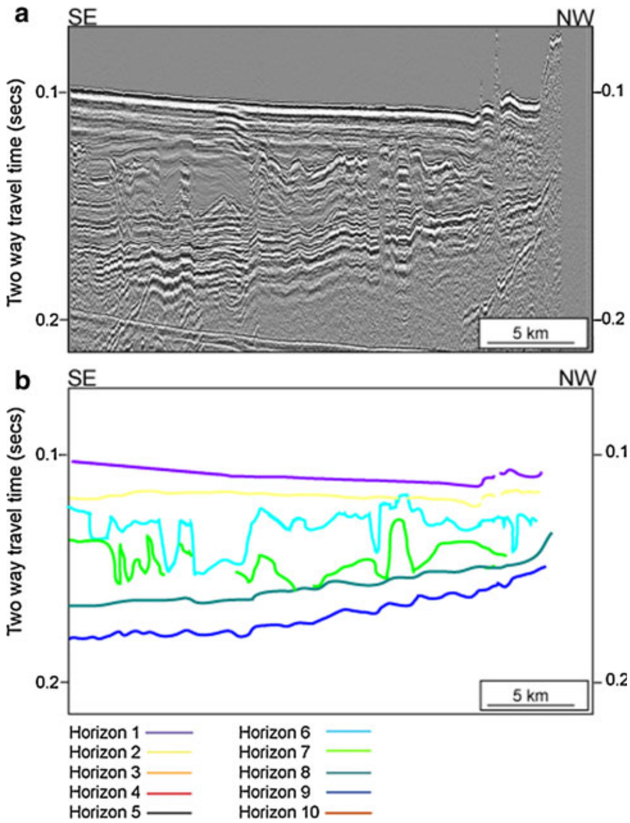


**Fig. 8** **a** Image of Line 8 seismic showing channelization of Horizon 6, more deformation and a series of protrusions, possible reefs at the surface. **b** Interpretation of Line 8 showing zones reef development and channel formation. Deformation is also visible beneath Horizon 9. See Fig. 2 for location

(Fig. 7) in particular shows a distinct channel cutting through the highly deformed sequence. These channels run both parallel and perpendicular to the shelf.

## Discussion

### Controls on sedimentation

We mapped 10 unconformities on the western Indus Shelf and across the continental margin. Table 1 provides detailed descriptions of all 10 horizons and facies observed during this study and the distribution of each horizon is shown in Fig. 9. All horizons show a deepening toward the southwest, which would be expected as the shelf break is reached, and a smooth distribution across the shelf, suggesting spatial consistency in the processes that produced the horizons. However, Horizons 1–4 also appear deeper (>0.3 s) in the east of the study area near the Indus Canyon, probably related to slumping. Older horizons (e.g. Horizon 9) appear shallow in the northwest of the survey area close to the coast. This is probably related to the uplift. At least on the shelf these are erosional surfaces, so we are confident in interpreting them as lowstand horizons. During a sea level cycle erosion surfaces can form during a marine transgression and through subaerial exposure. Subaerial exposure often leads to the formation of gullies or larger canyons, depending on the length of exposure (e.g., Posamentier and Allen 1993). Erosion surfaces can also form during marine transgressions as the focal point of erosion retreats landwards in response to the sea level rise, creating a flooding or ravinement surface (e.g., Stamp 1921; Kraft 1971; Walker and Eyles 1991; Lantzsch et al. 2010). Such features often occur across large swaths in sedimentary basins (Walker and Eyles 1991; Cattaneo and Steel 2003). Several horizons such as Horizons 1, 6, and 7 show extensive channelization either on the inner shelf and/or near the shelf edge and are probably linked to exposure. The remaining horizons could be related to marine transgressions or could represent migration of depositional lobes during the switching of the delta.

Similar erosion surfaces to Horizons 2, 3, 4, 5, 6, 8, 9 and 10 have been documented elsewhere and been linked to lobe switching (e.g., Allison et al. 2000; Draut et al. 2005; Corregiani et al. 2005; Xue et al. 2010). Many of the thick sedimentary packages discussed between these horizons do occur close to the shelf edge, where thick lobes can accumulate under high sediment supply (Porebski and Steel 2006). However, even under high sediment supply major avulsion events may not be possible in confined basins subject to local deformation (Perov and Bhattacharya 2006). The Indus River is thought to have avulsed around the delta during the Holocene and many paleochannels within the delta region have been documented (Holmes 1968). However, unlike the Mississippi–Atchafalaya system a major lobate system has not developed in the Western Indus Shelf during the Holocene because of high deep water wave energy and insufficient sediment supply to match sea level rise. However, this may not have been the case prior to the Holocene. If lobe switching has occurred on the Indus Shelf then erosion surfaces could form without any local tectonic forces or changes in sea level and some of these partially preserved lobes have since been deformed by more recent tectonic events.

Between the unconformities the sedimentary record is dominated by a series of clinoforms that are generally best preserved towards the shelf edge (e.g., Figs. 3d, 4c) but are also found in deeper water on the upper slope (e.g., Fig. 6c).

Horizon 1 is the youngest unconformity, and is observed shelf-wide, so we interpret this to represent erosion at the last glacial maximum (LGM). Towards the coastline this is the base for the modern Indus Delta. Line P shows clinoformal morphology at its inshore end. Elsewhere sediment thickness above Horizon 1 is <17 m, as calculated using the stacking-derived velocities for depth conversion.

**Table 1** Description of (a) horizons and (b) facies types for the study area

| Unconformity name | Colour | Description | Example |
|---|---|---|---|
| *a* | | | |
| Horizon 1 | Purple | Very high amplitude reflector, angular base Huge variation in sediment thickness above | Line P (Fig. 3) |
| Horizon 2 | Light Yellow | Moderate amplitude, forms erosive surface on slopes. Sometimes channelled nearer coast | Line J (Fig. 5) |
| Horizon 3 | Orange | Moderate amplitude, forms erosive surface | Line I (Fig. 4) |
| Horizon 4 | Red | Moderate amplitude similar to Horizon 3 but broader | Line P (Fig. 3) |
| Horizon 5 | Black | High amplitude reflector forming a slump in the northwestern shelf | Line J (Fig. 5) |
| Horizon 6 | Light Blue | High amplitude Forms an erosive surface above zone of deformation | Line 10 (Fig. 7) |
| Horizon 7 | Bright Green | Forms base of a persistent western clinoform Moderate amplitude | Line P (Fig. 3) |
| Horizon 8 | Blue-Green | Highly channelized on western slope Smooth near coast Moderate amplitude | Line I (Fig. 4) |
| Horizon 9 | Dark Blue | V high amplitude No channels | Line K (Fig. 6) |
| Horizon 10 | Brown | Moderate amplitude associated with faulting | Line K (Fig. 6) |

| Facies types | Description | Examples |
|---|---|---|
| *b* | | |
| Channel fill | Occasionally steep sided, mostly between Horizon 2 and 6 on shallow slope in either orientation | Line 8 Figure 8 |
| Clinoforms | Erosive bases downslope, occasionally angular occur in many horizons | Line J Figure 5 |
| Diapir structure | Smooth uplifted dome like features occasionally penetrating seafloor | Line 8 Figure 8 |
| Domes | Deep broad features below 0.2 TWT located throughout downslope sections. Characterized by thin sedimentation subsequent fanning away for the modern shoreline | Line P Figure 3 |
| Slope channels | Steep angular channels at the top of the slope perpendicular to shelf | Line J Figure 5 |
| Sediment waves | Climbing stepped profile on slope beneath Horizon 2 | Line I Figure 4 |

There are two possible explanations for the wave-like features forming on the slopes (e.g., Line I; Fig. 4c, e): either they are small-scale faults caused by mass-movement events, or they are climbing sand waves caused by strong northwest to southeast bottom currents. Although a potential failure plane can be identified at the base of the upper unit, above Horizon 3 (Fig. 4c), the fact that the size of these structures decreases down slope strongly argues in favour of these being migrating sediment waves (Lee et al. 2002).

Tectonic deformation increases north-westward within the study region, shown both in the folding of sediments beneath Horizon 6 (Figs. 6d, 7), and in the domed structures of the picked horizons; Horizons 7–10 are shallow close to the coastline in the north, such as seen in Lines I, and 8, while Horizons 3–10 show relative deepening of the shelf edge in the north of the survey area. There is also localised deepening of individual horizons towards the coastline, indicating preferential sediment storage on that part of the shelf. Unfortunately, accurately dating the ages of these unconformities is difficult, if not impossible, because no complete age model for the Pleistocene has been produced for the offshore Indus region because of a lack of appropriate drilling/coring. This is a research task that needs to be undertaken in the future in order to accurately date the ages of these clinoforms.

## Sediment supply

Recent sedimentation is unevenly distributed across the shelf: Since the LGM, shelf sedimentation has been focused on the eastern region of the shelf with thinner sediments elsewhere and a small modern clinoform west of the canyon (Giosan et al. 2006), which is only present on the north-eastern, coastal side of the western shelf. This is consistent with the observations of von Rad and Tahir

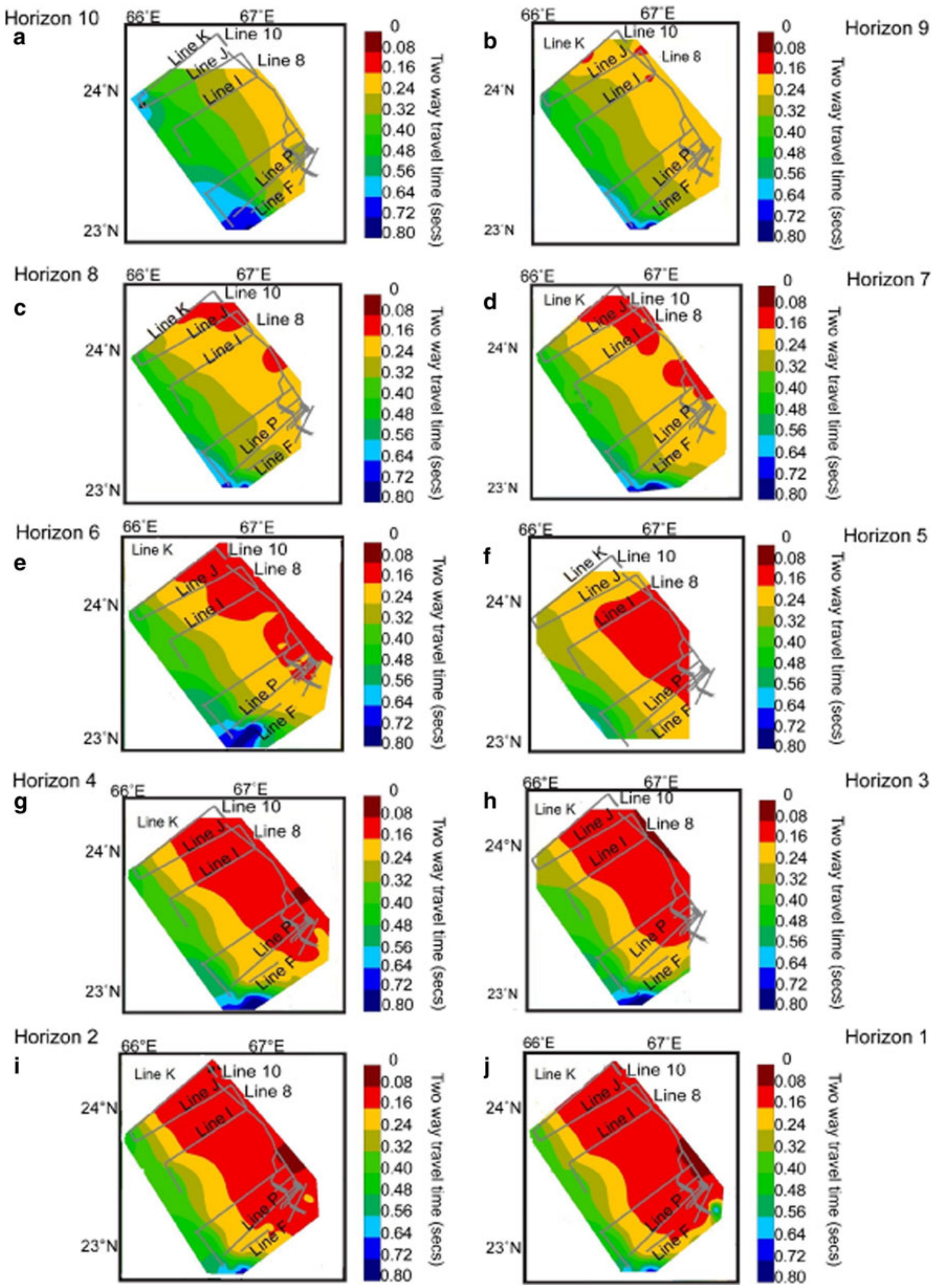


**Fig. 9** Horizon map for each of the 10 western shelf horizons. **a** Horizon 10, **b** Horizon 9, **c** Horizon 8, **d** Horizon 7, **e** Horizon 6, **f** Horizon 5, **g** Horizon 4, **h** Horizon 3, **i** Horizon 2, **j** Horizon 1. This shows a general thickening of sediment towards the northwest

(1997) of a mud drape forming during the Holocene on the shelf west of the Indus Canyon and suggests that supply to the western shelf has been restricted during and after the most recent sea level rise.

It is not certain when the older clinoforms developed, and their incomplete preservation makes it difficult to assess their detailed architecture. Prograding deltaic clinoforms can form in response to falling sea level (e.g., Hanebuth et al. 2002; Ridente et al. 2009), even on shelves with only moderate sediment supply (Porebski and Steel 2006). Alternatively the clinoforms on the Indus Shelf may form during highstands. This is clearly the case now, since the modern clinoform is prograding from the coastline, but has had insufficient time to prograde to the modern shelf edge, despite the long duration of the Holocene compared to most interglacials. If clinoforms are incapable of reaching the shelf edge during this long interglacial then it seems less likely that the shelf edge deltas/clinoforms seen underlying the present system were formed during high stands alone. More likely they represent sedimentation when sea level was close to the shelf edge, probably during a period of falling sea level. During prolonged lowstands these newly formed clinoforms are also partially eroded before being buried by a new deltaic clinoform prograding to the shelf edge. Over time periods of $>10^5$ years the Indus delivers the majority of its load to the Indus Canyon and the deep ocean (Naini and Kolla 1982). However, our interpretation implies that during highstands the bulk of the Indus River load is stored on the shelf. While some material may reach the upper canyon, coring on the upper fan demonstrates that sediment transport is not reaching the deep sea in significant amounts (Prins et al. 2000).

Gullies have formed around the shelf break as result of mass wasting. Our seismic data demonstrate that erosive channels are common features of lowstands during the Pleistocene across the shelf (e.g., Line 10, Fig. 7). These could act as mechanism for moving large quantities of sediment down the slope. We have produced a series of isopach maps based on the most widely picked regional seismic reflectors in order to map out the general patterns of sediment preservation on the shelf through time (Fig. 10a–g). Prior to the LGM (Fig. 10a–f) the thickest part of many of the sequences lies at the shelf break because this is where the greatest accommodation space existed, contrasting with regions where the shelf was experiencing tectonic uplift. Alternatively this thickening at the shelf edge may reflect faster erosion rates on the shelf during lowstands or reworking during marine transgression coupled with localised subsidence of the shelf, as shown by thicker sediment in Fig. 10e, f. In many cases the areas where sedimentation is thinnest is in the middle of the shelf (for example Fig. 10b), where we observe tectonically generated domes and folds. The fanning of sediment away

**Fig. 10 a–g** Isopach maps showing thickness of sediments since. ▶ Highest rates are currently in the east of the region (Fig. 10a) but in the past, sediment has accumulated at the shelf edge where relict clinoforms are present

from these domes is consistent with active structures beneath the shelf.

Isopach maps for selected intervals (Fig. 11) have been produced in order to show how sedimentation developed through time. Zones of deformation are also highlighted. Total accumulated sediment beneath the LGM surface increased seaward and across the shelf edge, with decreasing sedimentation and erosion in shallower water areas (Fig. 11a). Accumulation is particularly limited in the north because of the tectonically driven uplift of the shelf, restricting accommodation space. The more southern lines show uplift in the middle of the shelf and then thickening sediment landward. Between Horizons 6 and 9, 80-m-thick sediment has accumulated just inshore of the shelf edge in the northwest (Fig. 11d). This is where the seismic profiles show tilting (e.g., Line K, Fig. 6d).Together these patterns define a broad fold with an axis running northwest to southeast across the western shelf. Since at least the start of the Holocene sediment has gradually built up on the eastern half of the shelf (Fig. 11b), although where slumping has occurred sediment has still accumulated on the upper slope (Line I, Fig. 4c).

## Deformation under the western shelf

The interpretation of faults is based on the observation of small, straight displacements running through sections of the reflection data. We relate these faults to regional deformation. Compressional deformation appears strongest in the far northwest, where it is visible cutting through the whole succession, although significantly more is developed beneath Horizons 5 and 6. A series of tight folds is visible in the almost perpendicular Lines K and 10 (Figs. 6d, 7). We attribute this deformation to sinistral transpression along the Murray Ridge plate boundary, which has been linked previously to the formation of northwest to southeast trending folds and faults (Edwards et al. 2000; Carmichael et al. 2009). Furthermore, deep-penetrating growth faults are thought to exist across the western shelf and slope (Calvès et al. 2008). On the north-west Indus Fan and slope between 2 and 4 s (TWT) detached anticlines linked to the migration of fluids are observed (Calvès et al. 2008). It is possible that the dome features observed in our seismic data represent one of these anticlines, or are linked to the growth faulting. Unfortunately the resolution of the industry-standard seismic used by Calvès et al. (2008) is not sufficient to show evidence for deformation above 2 s (TWT). This is the first time that such anticlines features have been documented within the region outside the deeper-water Indus Fan.

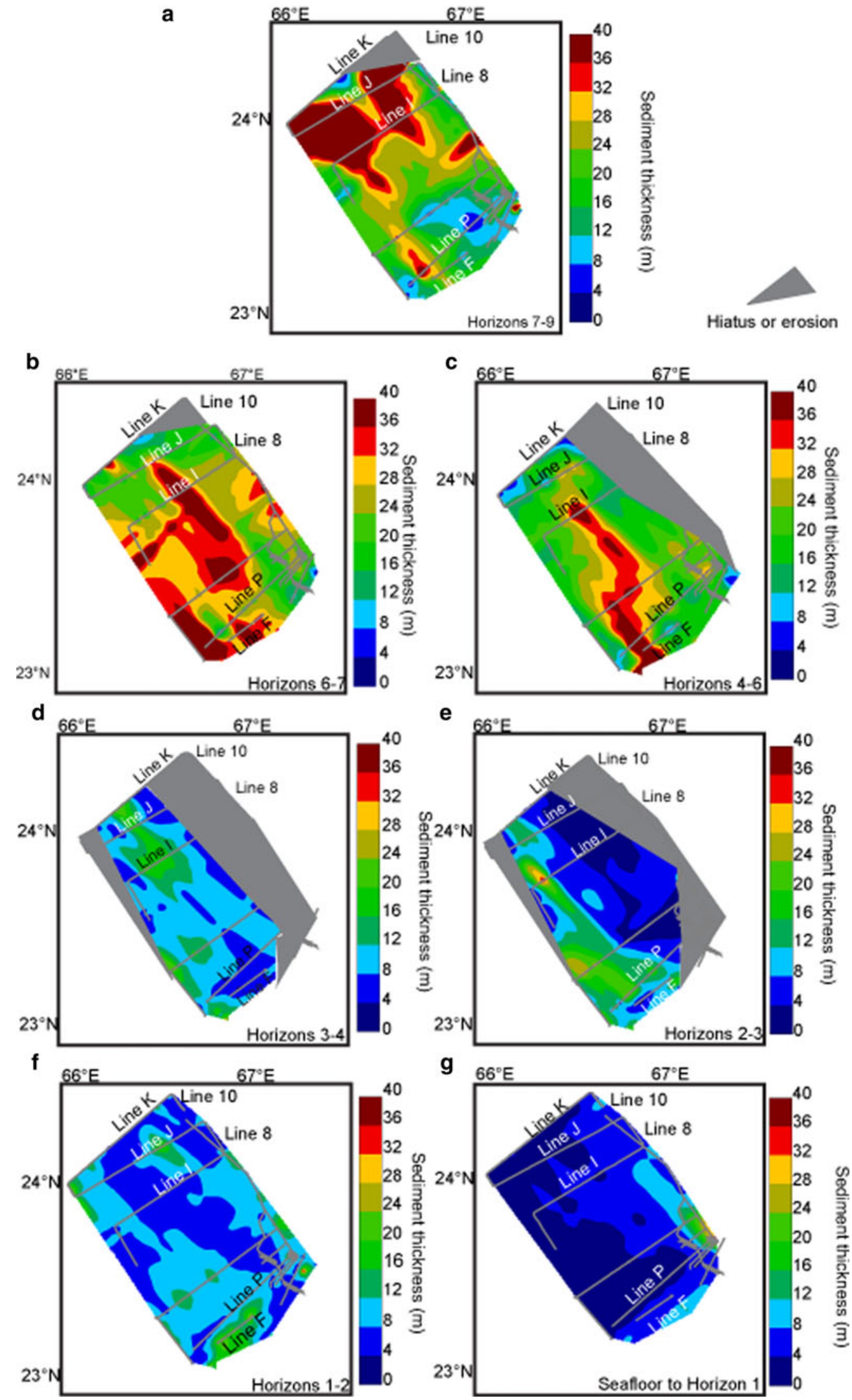
a
66°E
67°E
24°N
23°N
Line K
Line 10
Line 8
Line J
Line I
Line P
Line F
Horizons 7-9
40
36
32
28
24
20
16
12
8
4
0
Sediment thickness (m)
Hiatus or erosion
b
Horizons 6-7
c
Horizons 4-6
d
Horizons 3-4
e
Horizons 2-3
f
Horizons 1-2
g
Seafloor to Horizon 1

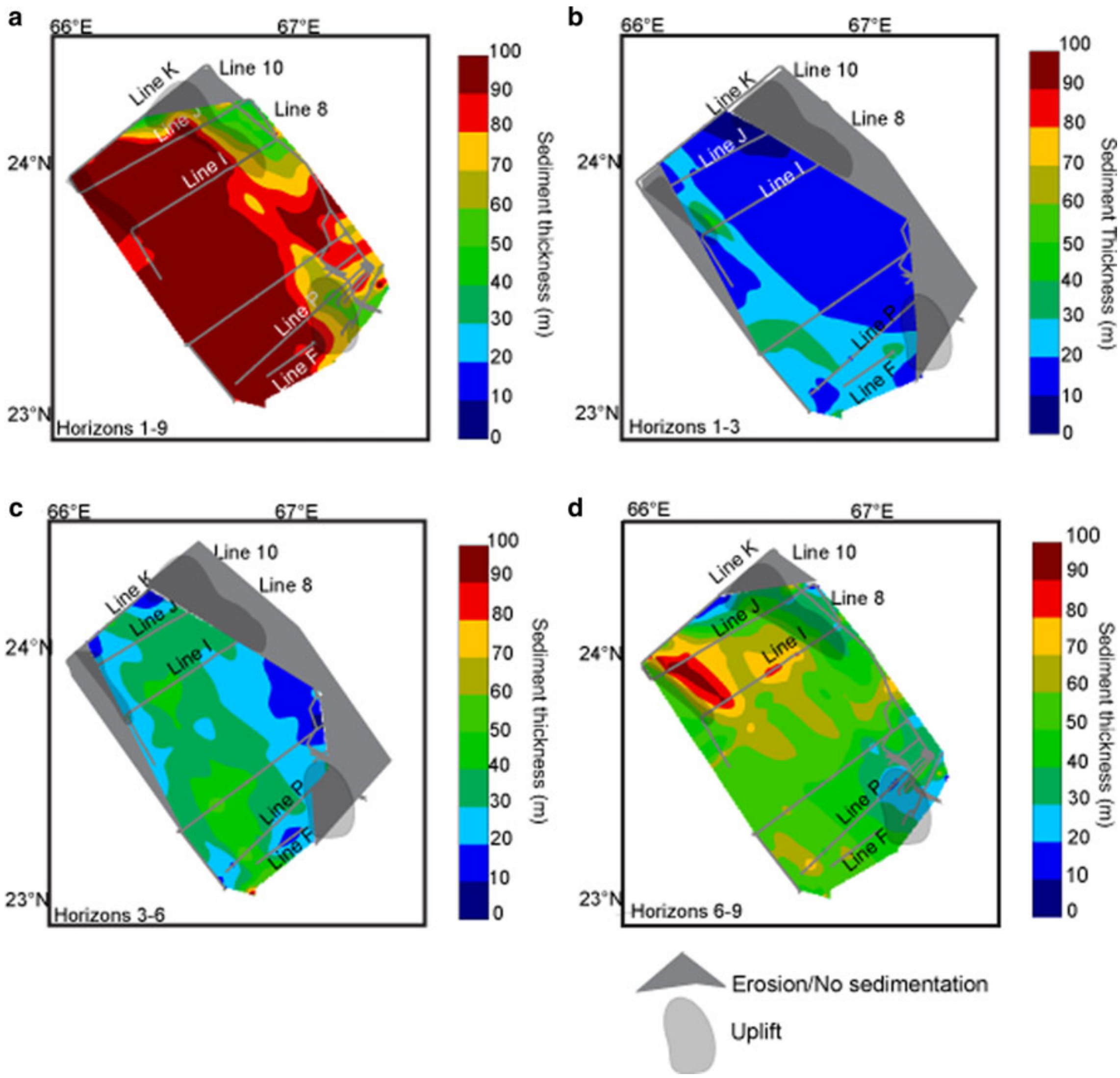


**Fig. 11** Isopach maps for selected horizon intervals **a** Horizons 1–9, **b** Horizons 1–3, **c** Horizons 3–6, **d** Horizons 6–9. Regions of uplift are also shown. Sedimentation in more recent times appears more focused away from the shallower regions and instead occurs on the slope

Changes in regional base level driven by tectonic deformation exert a strong control on sedimentation and sediment preservation. A clinoform between Horizons 6 and 7 (Figs. 4d, 10) has developed by prograding from a broad zone of uplift, a pattern that is traceable across much of the western shelf. The clinoform does appear to reduce in size towards the west, suggesting a structure of significant length and sediment supply across the shelf. In the central western shelf, where only one dome feature is observed this appears to result in a progradation sequence, such as that seen in Lines F and P (Figs. 2, 3). In the far northwest the structures on Line K (Fig. 6e) are most easily explained by further folding developed offshore of the shelf edge around the time of Horizon 6. Models of shelf development for the western region of the shelf (Fig. 12) show how the region may have looked during different time intervals. At the time of formation of Horizon 6 (Fig. 12a) when the domes on the slope appear to have been more active than at present sediment fill occurs principally along the slope, although if sediment supply rates were too low, some sediment accumulated landward of these domes. Prior to the development of the modern clinoform (Fig. 12b), clinoform development appears to have been focused over these dome features, though whether this is linked entirely to clinoforms closer to the shoreline is unclear.

## Conclusions

The Indus Shelf has undergone complex development during the Quaternary, resulting in a series of stacked

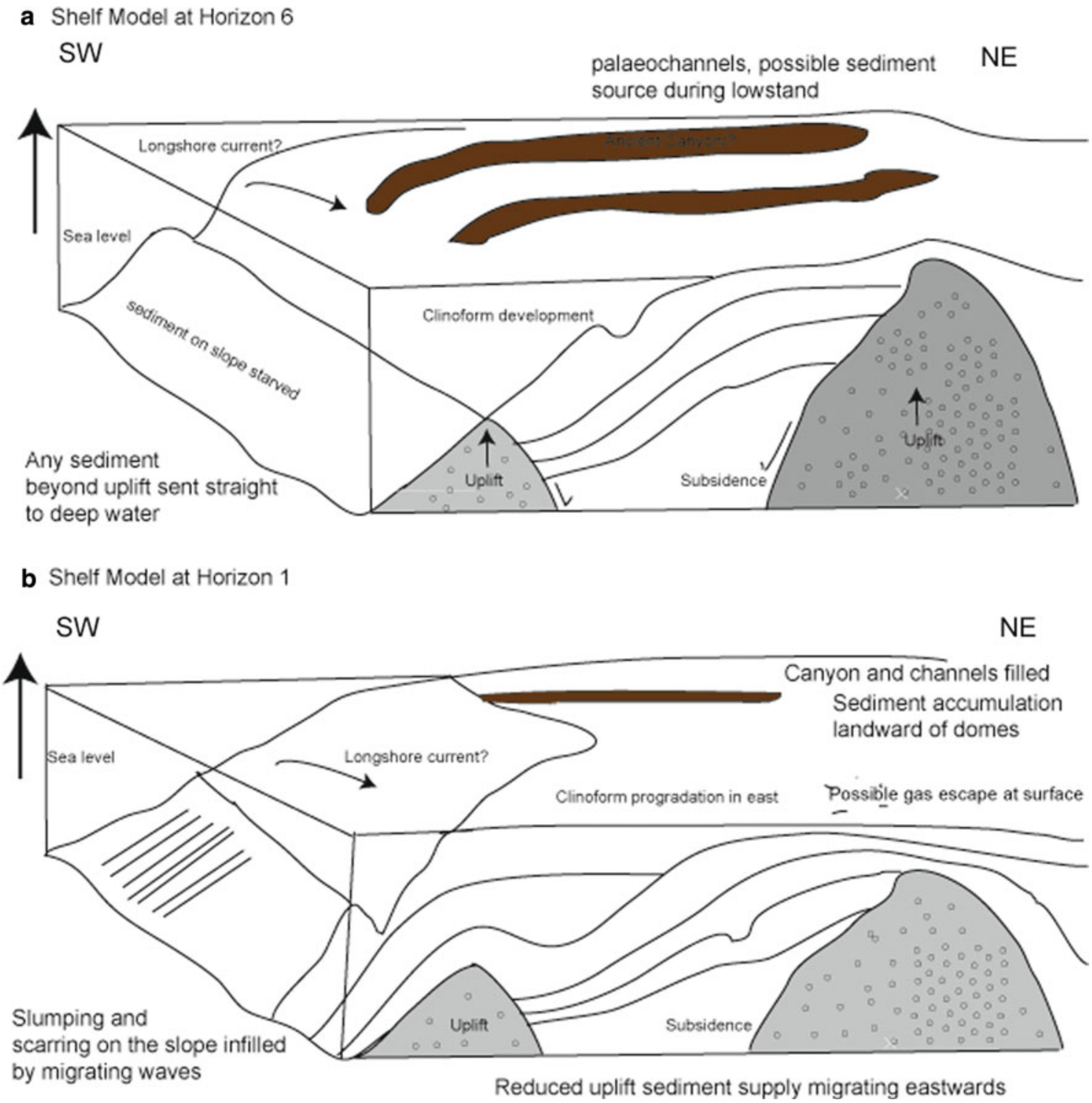


**Fig. 12** Schematic model of shelf sedimentation at **a** Horizon 6, **b** Horizon 1 before the development of the modern clinoform. Clinoforms appear to have prograded further across the slope, presumably as result of less uplift and subsidence

clinoforms on the western Indus Shelf. The precise shape of the clinoforms is a function of the competing influences of sediment supply, tectonic deformation, and sea level change. We suggest that most of the clinoforms, which formed close to the shelf edge, developed during periods of falling sea level and could be partly caused by lobe switching. Sediment thickness is affected by deformation beneath the western shelf. Dome structures (anticlines) observed under the mid shelf are linked to transpression along the Murray Ridge plate boundary and are important in restricting total sediment thickness in that region. Subsidence of the strata next to these dome features has created accommodation space for the development of prograding clinoform sequences during highstands before each package was eroded during the following sea level fall. Since the Last Glacial Maximum the dominant sediment-transport direction has shifted to the eastern part of the Western Shelf, where a prominent clinoform is observed close to the shelf edge while sediment supply has been decreasing to the west.

**Acknowledgments** DL would like to thank all the participants of Pelagia cruise 64PE300, especially the captain, crew and shore-support staff at NIOZ and NOC Southampton. DL was supported by a studentship grant NE/G002029/1. DL also thanks Luke Pinson, Mark Vardy, David Iacopini, Huw Llewellyn and Ron Steel for useful discussions. The work was greatly improved by three reviewers and the editor. This work was also funded by Natural Environment Research Council (UK) grant NE/D005442/1. Contributions by LG and CP were funded by NSF-OCE 0623766 to LG. We thank the government of Pakistan and the Director of the National Institute of Oceanography for their cooperation in this study. PC thanks the Hanse Wissenschaftskollog, Germany for providing time to think about these issues.

## References

Allison MA, Kineke GC, Gordon ES, Goñi MA (2000) Development and reworking of a seasonal flood deposit on the inner continental shelf of the Atchafalaya River. Con Shelf Res 20:2267–2294. doi:10.1016/S0278-4343(00)00070-4

Burgess PM, Hovius N (1998) Rates of delta progradation during highstands: consequences for timing of deposition in deep marine systems. J Geol Soc 155:217–222

Calvès G, Huuse M, Schwab A, Clift P (2008) Three-dimensional seismic analysis of high-amplitude anomalies in the shallow subsurface of the Northern Indus Fan: sedimentary and/or fluid origin. J Geophy Res 113:B11103. doi:10.1029/2008JB005666

Carmichael SM, Akhter S, Bennett JK, Fatimi MA, Hosein K, Jones RW, Longacre MB, Osborne MJ, Tozer RSJ (2009) Geology and hydrocarbon potential of the offshore Indus Basin Pakistan. Petrol Geosci 15:107–116. doi:10.1144/1354-079309-826

Cattaneo A, Steel RJ (2003) Transgressive deposits: a review of their variability. Earth Sci Rev 62:187–228. doi:10.1016/S0012-8252(02)00134-4

Clift P (2006) Controls on the erosion of Cenozoic Asia and the flux of clastic sediment to the ocean Earth Planet. Sci Lett 241:571–580. doi:10.1016/j.epsl2005.11.028

Clift PD, Shimizu N, Layne GD, Gaedicke C, Schlüter HU, Clarke M, Amjad S (2001) Development of the Indus Fan and its significance for the erosional history of the Western Himalaya and Karakoram. Bull Geol Soc Am 113:1039–1051. doi:10.1130/0016-7606(2001)113<1039:DOTIFA>2.0.CO;2

Clift P, Gaedicke C, Edwards R, Lee J II, Hildebrand P, Amjad S, White RS, Schlueter H-U (2002) The stratigraphic evolution of the Indus Fan and the history of sedimentation in the Arabian Sea. Mar Geophys Res 23:223–245. doi:10.1023/A:1023627123093

Corregiani A, Cattaneo A, Trincardi F (2005) The modern Po Delta system: lobe switching and asymmetric prodelta growth. Mar Geol 222:49–74. doi:10.1016/j.margeo.2005.06.039

Coumes F, Kolla V (1984) Indus Fan: seismic structure, channel Migration and sediment-thickness in the Upper Fan. In: Haq BU, Milliman JD (eds) Marine geology and oceanography of Arabian Sea and Coastal Pakistan. Von Nostrand Reinhold Company, New York, pp 101–110

Daley T, Alam Z (2002) Seismic stratigraphy of the offshore Indus Basin. In: Clift PD, Kroon D, Gaedicke C, Craig J (eds) The tectonic and climatic evolution of the Arabian Sea. Geological Society, Lond spec publ, pp 259–271. doi:10.1144/GSL.SP.2002.195.01.14

Deptuck ME, Steffens GS, Barton M, Pirmez C (2003) Architecture and evolution of upper fan channel-belts on the Niger Delta slope and in the Arabian Sea Mar Petrol Geol 20:649–676. doi:10.1016/j.marpetgeo.2003.01.004

Draut A, Kineke GC, Velasco DW, Allison MA, Prime RJ (2005) Influence of the Atchafalaya River on the recent evolution of the chernier-plain inner continental shelf, northern Gulf of Mexico Con. Shelf Res 25:91–112. doi:10.1016/j.csr.2004.09.002

Droz L, Bellaiche G (1991) Seismic facies and geologic evolution of the central portion of the Indus Fan. In: Weimer P, Link MH (eds) Seismic facies and sedimentary processes of submarine fans and turbidite systems. Springer, Berlin, pp 383–402

Edwards RA, Minshull TA, White RS (2000) Extension across the Indian-Arabian plate boundary: the Murray Ridge. Geophys J Int 142:461–477. doi:10.1046/j.1365-246x.2000.00163

Gaedicke C, Schlüter H-U, Roeser HA, Prexl A, Schreckenberger B, Meyer H, Reichert C, Clift P, Amjad S (2002) Origin of the northern Indus Fan and Murray Ridge, Northern Arabian Sea: interpretation from seismic and magnetic imaging. Tectonophysics 355:127–143. doi:10.1016/S0040-1951(02)00137-3

Giosan L, Constantinescu S, Clift PD, Tabrez AR, Danesh M, Inam A (2006) Recent morphodynamics of the Indus shore and shelf Con. Shelf Res 26:1668–1684. doi:10.1016/j.csr.2006.05.009

Greene DL, Rodriguez AB, Anderson JB (2007) Seaward-branching coastal-plain and Piedmont incised-valley systems through multiple sea-level cycles: late Quaternary examples from Mobile Bay and Mississippi Sound, USA. J Sed Res 77:139–158. doi:10.2110/jsr.2007.016

Hanebuth TJJ, Stattegger K, Saito Y (2002) The stratigraphic architecture of the central Sunda Shelf (SE Asia) recorded by shallow-seismic surveying. Geo Mar Letts 22:86–94. doi:10.1007/s00367-002-0102-1

Haq BU, Hardenbol J, Vail PR (1987) Chronology of fluctuating sea levels since the Triassic. Science 235:1156–1167

Henriksen S, Hampson GJ, Helland-Hansen W, Johannessen EP, Steel RJ (2009) Shelf edge and shoreline trajectories, a dynamic approach to stratigraphic analysis. Basin Res 21:445–453. doi:10.1111/j.1365-2117.2009.00432.x

Holmes DA (1968) The Recent History of the Indus. Geogr J 134:367–382

Jelgersma S, Van der Zijp M, Brinkman R (1993) Sea level rise and the coastal lowlands in the developing world. J. Coast Res 9:958–972

Kazmi AH (1984) Geology of the Indus Delta. In: Haq BU, Milliman JD (eds) Marine geology and oceanography of Arabian Sea and Coastal Pakistan. Von Nostrand Reinhold Company, New York, pp 71–84

Kolla V, Coumes F (1987) Morphology, internal structure, seismic stratigraphy and sedimentation of the Indus fan. AAPG Bull 71:650–677

Kraft JC (1971) Sedimentary facies patterns and geologic history of a Holocene marine transgression. Geol Assoc Amer Bull 82:2131–2158

Lantzsch H, Hanebuth TJJ, Heinrich R (2010) Sediment recycling and adjustment of deposition during drowning a low-accumulation shelf (NW Iberia). Con Shelf Res 30:1665–1679. doi:10.1016/j.csr.2010.06.013

Lee HJ, Syvitski JPM, Parker G, Orange D, Locat J, Hutton EWH, Imram J (2002) Distinguishing sediment waves from slope failure deposits: field examples including the 'Humbolt Slide' and modelling results. Mar Geol 192:79–104. doi:10.1016/S0025-3227(02)00550-9

McHargue TR (1991) Seismic facies processes and evolution of Miocene inner fan channels, Indus submarine fan. In: Weimer P, Link MH (eds) Seismic facies and sedimentary processes of submarine fans and turbiditic systems. Springer, New York, pp 403–413

Milliman JD, Syvitski JPM (1992) Geomorphic/tectonic control of sediment discharge to the ocean: the importance of small mountainous rivers. J Geol 100:525–544

Milliman JD, Quiraishee GS, Beg MAA (1984) Sediment discharge from the Indus River to the Ocean: past, present, future. In: Haq BU, Milliman JD (eds) Marine geology and oceanography of Arabian Sea and Coastal Pakistan. Von Nostrand Reinhold Company, New York, pp 65–70

Naini B, Kolla V (1982) Acoustic character and thickness of sediments of the Indus Fan and the continental margin of western India. Mar Geol 47:181–195

Perov G, Bhattacharya JP (2006) Pleistocene shelf-margin delta: Intra deltaic deformation and sediment bypass, northern Gulf of Mexico. AAPG Bull 95:1617–1641. doi:10.1306/01271109141

Pinson LJW (2010) Remote classification of sediment properties using high-resolution marine seismic data. PhD thesis, School of Ocean and Earth Science, University of Southampton, UK, 2010

Porebski SJ, Steel RJ (2006) Deltas and Sea level change. J Sed Res 76:390–403. doi:10.2110/jsr.2006.034

Posamentier HW, Allen GP (1993) Variability of the sequence stratigraphic model: effects of local basin factors Sed Geol 86:91–109

Pratson LF, Nittrouer CA, Wilberg P, Steckler MS, Swenson JB, Cacchione DA, Karson JA, Murray AB, Wolinsky MA, Gerber TP, Mullenbach BL, Spinelli GA, Fulthorpe CS, O'Grady DB, Parker G, Driscoll NW, Burger RL, Paola C, Orange DL, Field ME, Friedrichs CT, Fedele JJ (2007) Seascape evolution on clastic continental shelves and slopes. In: Nittrouer CA, Austin JA, Field ME, Kravitz JH, Syvitski JPM, Wilberg P (eds) Continental Margin Sedimentation Int Assoc Sed special pub., pp 339–381. doi:10.1002/9781444304398.ch7

Prins MA, Postma G, Cleveringa J, Cramp A, Kenyon NH (2000) Controls on terrigenous sediment supply to the Arabian Sea during the late Quaternary: the Indus Fan. Mar Geol 169:327–349. doi:10.1016/S0025-3227(00)00086-4

Reijenstein HM, Posamentier HW, Bhattacharya JP (2011) Seismic geomorphology and high-resolution seismic stratigraphy of inner-shelf fluvial, estuarine, deltaic, and marine sequences, Gulf of Thailand. AAPG Bull 95:1959–1990. doi:10.1306/03151110134

Ridente D, Trincardi F, Piva A, Asioli A (2009) The combined effect of sea level and supply during Milankovitch cyclicity: evidence from shallow-marine $\delta^{18}$O records and sequence architecture (Adriatic Margin). Geology 37:1003–1006. doi:10.1130/G25730A.1

Siddiqui MN, Maajid S (2004) Monitoring of geomorphological changes for planning reclamation work in coastal area of Karachi. Pakistan Adv Space Res 33:1200–1205. doi:10.1016/S0273-1177(03)00373-9

Sirocko F, Lange H (1991) Clay mineral accumulation rates in the Arabian Sea during the Late Quaternary. Mar Geol 97:105–119. doi:10.1016/0025-3227(91)90021-U

Stamp LD (1921) On cycles of sedimentation in the Eocene strata of the Anglo-Franco-Belgian Basin. Geol Mag 58:108–114

Swenson JB, Paola C, Pratson L, Voller VR, Murray AB (2005) Fluvial and marine controls on combined subaerial and subaqueous delta progradation: morphodynamics modeling of compound clinoform development. J Geophys Res 110:F201. doi:10.1029/2004JF000265

Vail PR, Mitchum RM, Todd RG, Widmier JM, Thompson SI, Sangree JB, Bubb JN, Hatlelid WG (1977) Seismic stratigraphy and global changes of sea-level. In: Payton CE (ed) Seismic stratigraphy—applications to hydrocarbon exploration. Memoir, vol 26. American Association of Petroleum Geologists, Tulsa pp 49–212

von Rad U, Tahir M (1997) Late Quaternary sedimentation on the outer Indus Shelf and slope (Pakistan): evidence form high-resolution seismic data and coring. Mar Geol 138:193–236. doi:10.1016/S0025-3227(96)00090-4

Walker RG, Eyles CH (1991) Topography and significance of a basinwide sequence bounding erosion surface in the Cretaceous Cardium Formation, Alberta, Canada. J Sed Petrol 61:473–496

Wells JT, Coleman JM (1984) Delta morphology and sedimentology with special reference to the Indus River delta. In: Haq BU, Milliman JD (eds) Marine geology and oceanography of Arabian Sea and Coastal Pakistan. Von Nostrand Reinhold Company, New York, pp 85–100

Xue Z, Liu JP, DeMaster D, Van Nguyen L, Ta TKO (2010) Late Holocene evolution of the mekong subaqueous delta. Southern Vietnam Mar Geol 269:46–60. doi:10.1016/j.margeo.2009.12.005